

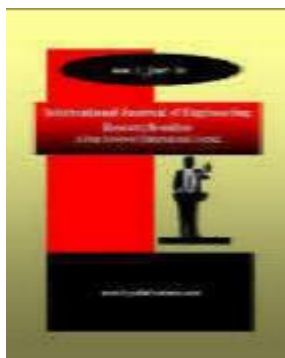
## RESEARCH ARTICLE

**MORPHOLOGY AND MAGNETIC PROPERTIES OF CADMIUM ION SUBSTITUTED NICKEL, ZINC NANO FERRITES**V V J GOPALA KRISHNA<sup>1</sup>, M.RAMA REDDY<sup>2</sup><sup>1</sup>Senior Lecturer in chemistry, Mrs A V N College, Visakhapatnam, Andhra Pradesh<sup>2</sup> SG Lecturer in chemistry, G.B.R College, Anaparthi, E.G. District., Andhra Pradesh

Article Received: 22/10/2013

Article Revised: 29/11/2013

Article Accepted: 30/12/2013

**ABSTRACT**

Cadmium ion ( $\text{Cd}^{2+}$ ) doping with nickel ferrite with general formula  $\text{Cd}_x\text{Ni}_{1-x}\text{Zn}_x\text{Fe}_2\text{O}_4$  ( $x = 0.0, 0.2, 0.4,$ ) (CNZ) has been prepared by using Sol-Gel method and citrate precursor. The prepared samples are characterized by the x-ray diffraction (XRD), SEM-EDS and FTIR techniques. The XRD data have been used to obtain lattice constants; average crystallite size, specific surface area, dislocation density and strain of the CNZ nanoferrites and B-H loop tracer were carried out on the sintered specimens to identify the magnetic properties. The average crystallite size calculated using Scherrer's formula was found to be in the nanometer range, its value varying from 37 nm to 42 nm. Magnetic hysteresis loops were traced and found that, due to the  $\text{Cd}^{2+}$ -ions substitution, the values of saturation magnetization  $M_s$  for the investigated samples were decreased, whereas the coercive field  $H_c$  increased.

©KY PUBLICATIONS

**Introduction**

Spinel nanoferrites are considered superior to other magnetic materials because they have low eddy current losses due to high electrical resistivity. The possibility of preparing ferrites at the nano-scale has extended the application in biotechnology as well as in medicines. With the striking feature of "ferrimagnetism" nanocrystalline ferrites have attracted special attention of researchers in the field of electronic technology. Spinel ferrites of the type  $\text{MFe}_2\text{O}_4$  attract several researchers because of their twin property of magnetic conductor and electric insulator. These materials are widely used in the electronic and electrical industries for the fabrication of devices and components such as high density magnetic core of read/write for the high speed tapes etc<sup>1</sup>. In recent years there has been considerable interest in the study of the properties of nano-sized ferrite particles because of their importance in the fundamental understanding of the physical properties as well as to their proposed applications for many technological purposes<sup>2</sup>. Zinc ferrite nanoparticles make it one of the most significant materials in the application research area of Nanoscience and engineering. Zinc ferrite exposes super paramagnetic behaviour among other ferrites<sup>3</sup>.

Cadmium substituted nickel ferrites are the important class of spinel ferrites<sup>4</sup>. According to crystal structure, nickel ferrite is an inverse spinel ferrite and possesses high electrical resistivity and low eddy current losses<sup>5</sup>. They are attractive because of their numerous specialized applications importance in Ferro fluids, magnetic drug delivery, Nano gadgets, sensors and hyper thermic for cancer treatment<sup>6</sup>. The structural and magnetic properties of spinel ferrites depend on the magnetic interaction and cation distribution in the two sub-lattices i.e. tetrahedral (A) and octahedral (B) lattice sites<sup>7</sup>. Cd substituted Ni-Zn ferrite nanoparticles were prepared by sol-gel method. The aim of this paper is to report and discuss the results of structural and magnetic properties of  $Cd_xNi_{1-x}Zn_xFe_2O_4$  particles with varying compositions ( $x = 0.0, 0.2, 0.4$ ) synthesized by Sol-gel method.

## Experimental

### Materials and method

The 3 samples ( $x = 0.0, 0.2, 0.4$ ), of CNZ spinel ferrite was prepared by sol-gel technique. All chemicals and solvents were AR grade or better purchased from Merck Co.Pvt Ltd and Sd. fine chemical used without any further purification. The stoichiometric amounts of metal nitrates viz. Cadmium nitrate ( $Fe(NO_3)_2 \cdot 4H_2O$ ) (>99%), nickel nitrate  $Ni(NO_3)_2 \cdot 6H_2O$ , Ferric Nitrate [ $Fe(NO_3)_3 \cdot 9H_2O$ ] and Zinc Nitrate –  $Zn(NO_3)_2 \cdot 6H_2O$ , Citric acid - ( $C_6H_8O_7 \cdot H_2O$ ) used as starting materials for the synthesis. Metal nitrates in required proportions were dissolved in a minimum quantity of distilled water and mixed together. Aqueous solution of Citric acid was then added to the mixed metal nitrate solution (with and without Lanthanum nitrate). Ammonia solution was then added with constant stirring by maintaining the neutral pH (7.0). The solutions were heated at 90°C under continuously stirring to remove the excess of the solvent. By raising the temperature up to 200°C lead the ignition of gel. The dried gel burnt completely in a self-propagating combustion manner to form powder like substance. The burnt powder was ground in Agate Mortar and Pestle to get a fine Ferrite powder. Finally the burnt powder was calcined in air at 700°C temperature for 2 hours and cooled to room temperature.

### Characterizations

The structural characterization was made through X-ray diffraction (XRD) technique in the  $2\theta$  range of  $20^\circ - 80^\circ$ . The XRD pattern was recorded at room temperature using  $Cu-K\alpha$   $\lambda = 1.5406 \text{ \AA}$  radiation. The magnetic measurements were carried out at room temperature using pulse field magnetic hysteresis loop tracer. The morphology, structure and elemental composition of the sample were characterized by Scanning electron microscopy (SEM) and Energy dispersive X-ray spectra (EDS). FTIR spectra were recorded from  $400 \text{ cm}^{-1}$  to  $4000 \text{ cm}^{-1}$  for all the samples by taking KBr and sample in the ratio 99:1 respectively at room temperature.

## RESULTS AND DISCUSSION

### X-Ray Diffraction Study of NPs

X-ray diffraction patterns of CNZ spinel ferrites were recorded with the X-ray diffractometer (Philips). XRD of all samples were recorded in the  $2\theta$  range of  $20-80^\circ$  with  $Cu-K\alpha$  radiation ( $\lambda = 1.50405 \text{ \AA}$ ) at room temperature. The XRD patterns of the  $Cd_xNi_{1-x}Zn_xFe_2O_4$  ( $x = 0.0, 0.2, 0.4$ ) bulk is shown in Figure (1). The X-ray diffraction appearance of all samples the single phase of cubic spinel structure which agrees with result of<sup>8</sup>. The existence of Miller indices conforms (220), (311) and (400) major lattice plane and uncovers the cubic spinel phases that is specified by the reference of powders diffraction files as shown in Table 1. The structure and their crystallite size were evaluated. The crystallite size of the nano-crystalline samples was measured using Debye Scherer formula<sup>9</sup>,

$$D_{XRD} = 0.98\lambda/\beta \cos \theta \dots (1)$$

Where  $\lambda$  is the wavelength of X-ray used in  $\text{\AA}$ ,  $\beta$  is the full width at half-maximum (FWHM) in radians in the  $2\theta$  scale,  $\theta$  is the Bragg angle,  $D_{XRD}$  is the crystallite size in nm. The value of  $D$  decreases from 42 to 38 nm on increasing value of  $x$ . This can be attributed to the liberation of latent heat of surface which rises the local temperature, consequently slowing down the growth process and lowering ferrite concentration in the vicinity<sup>10</sup>. The X-ray density depends on the lattice parameters and molecular weights of the samples and the

values increase with increasing of Cd content, while particles size decreases with increasing of Cd content. The average crystallite size has been calculated from the full width at half maximum of the reflection and using the Scherer's formula equation 1

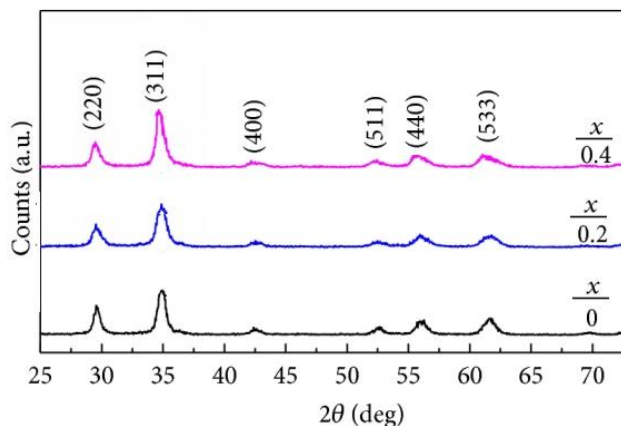


Fig. 1 X-ray diffraction pattern for CNZ nanoparticles at various concentrations

The lattice constant (a) was computed using the 'd' value and with their respective (hkl) parameters. Analysis of the diffraction pattern confirms the formation of cubic spinel structure for all the samples. The peaks indexed to (220), (311), (400), (511), (440) and (533) planes of a cubic unit cell, correspond to cubic spinel structure. The lattice constant calculated using the equation given below and tabulated in "Table 1"  $a = d(h^2 + k^2 + l^2)^{1/2}$

Table 1: Crystal & Magnetic Parameters of CNZ Ferrites for various concentrations of Cd<sup>2+</sup> ion

Concentration of Cd <sup>2+</sup> ion	Crystallite size (nm)	Lattice constant (Å)	D-spacing	X-ray density (g cm <sup>-3</sup> )	Magnetization (emu/g)	Coercivity (H <sub>c</sub> )	Magnetization Ms (emu/gm)
0.0	30.2547	8.102	2.514	6.254	21.8471	54.24	17.264
0.2	32.4069	8.321	2.534	6.984	20.6487	50.27	16.257
0.4	34.1024	8.423	2.569	7.021	18.9842	32.57	16.127

The lattice constant was found to increase from 8.102 to 8.42Å with increase in cadmium concentration, which is in good agreement with reference to Vegard's law (L.H. Gul et al 2008). The addition of cadmium displaces the Fe ions from tetrahedral to octahedral site and larger ionic radius of Cd (0.97Å) elongates the lattice. It is also observed that the sample with higher cadmium content has a larger lattice parameter. Similar variation of lattice constant is observed in the literature, when the ion of larger ionic radii is substituted in nickel ferrite<sup>11</sup>.

**FT IR Analysis**

FTIR spectra were recorded in the range of 400–4000 cm<sup>-1</sup> as shown in the Figures 2. The IR bands of solids are usually assigned to the vibrations of ions in the crystal lattice. Two main broad metal-oxygen bands are seen in the FTIR spectra of all ferrites in particular. Below 700 cm<sup>-1</sup> the octahedral-metal stretching vibration frequency (Oh)  $Mocta \leftrightarrow O [B \text{ site}]$  and 800-900 cm<sup>-1</sup> corresponds to intrinsic stretching vibrations of the metal at the tetrahedral site (Td)  $Mtetra \leftrightarrow O [A \text{ site}]$

In the FTIR spectrum of the samples, the band appears from 1098-1120 cm<sup>-1</sup>, which relates to lattice vibration of oxide ion against the cations. The bands in the region from 1300- 1700 cm<sup>-1</sup> are relates to both Symmetric & asymmetric C-O stretching frequency, and this may be due to the CO<sub>2</sub> adsorbed by the samples from atmosphere.

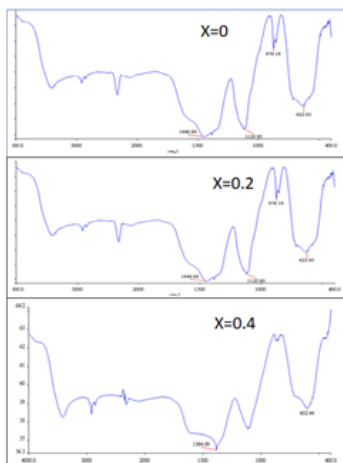


Figure 2: FTIR Spectra of  $Cd_xNi_{1-x}Zn_xFe_2O_4$  ( $x = 0.0, 0.2, 0.4$ ), nano ferrites

### SEM-EDX analysis

Micro structural analysis of the prepared samples was carried out by Scanning Electron Microscopy (SEM). The SEM micrographs of the prepared samples were shown in below figure 3. The SEM micrographs shows that the grains have almost homogeneous distribution and clusters between the particles. The grain size of the samples lies in the nano meter region have a spherical shape and narrow size distribution. SEM image revealed that with increasing in the Cd concentration, then the grain size has increased (except for  $x=0.4$ ) which is an evidence for the XRD analysis. One can see voids and pores in the samples. This observation could be attributed to the release of large amount gases during combustion process due decomposition.

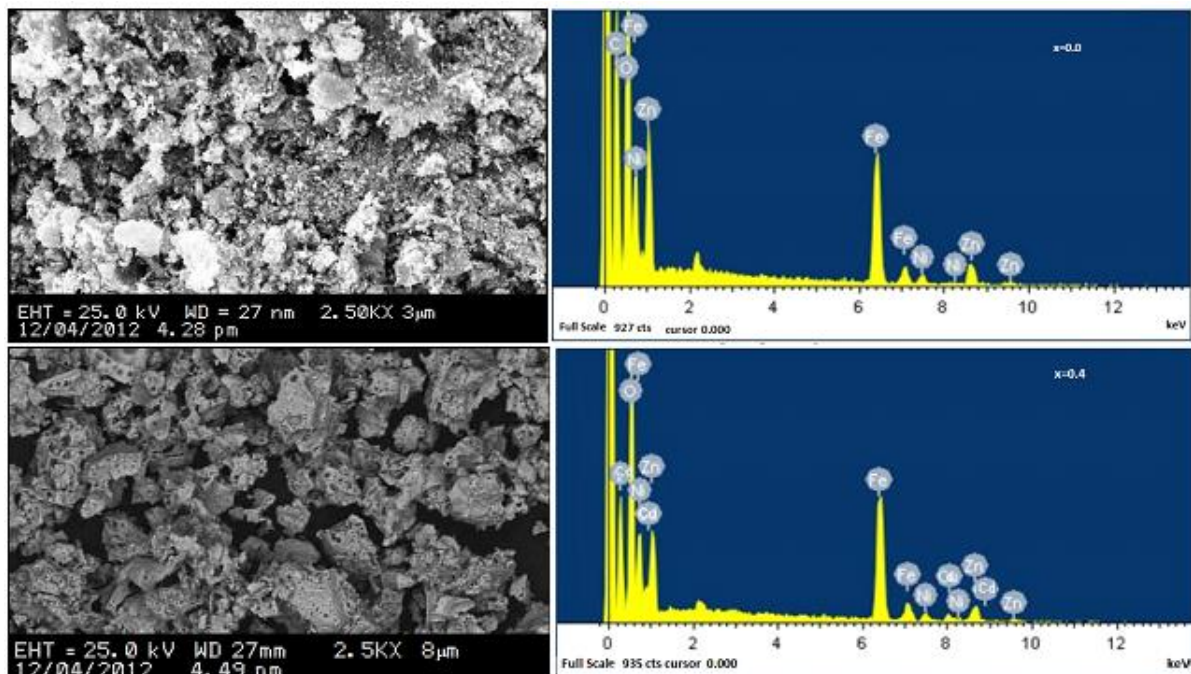


Figure 3: SEM Micrographs (Left) and EDS Spectra of  $Cd_xNi_{1-x}Zn_xFe_2O_4$  ( $x = 0.0$  &  $0.4$ ), nano ferrites

Energy dispersive X-ray (EDX) analysis of the as prepared specimen was carried out at  $x = 0$  and  $x = 0.4$  of Cadmium ion concentrations. This finding shows almost homogeneous and uniform distribution of Zn and Fe particles in the powder sample. The effective atomic concentration of Zn, Fe and oxygen species on top surface layers of the solid investigated are determined by EDX technique. The relative atomic abundance of Cd, Zn, Ni, Fe and O species present in the uppermost surface and bulk layers of Zn ferrite. This observation may

be reported to the increase in the mobility of Cd and Fe species with subsequent an increase in the formation of Cd ferrite. In addition that the surface concentrations of Cd, Zn, Fe and oxygen species at 20 keV on different areas over the surface of specimen studied are much closed to each other. This indicates the homogeneous distribution of Cd, Ni, Zn, Fe and O species in the investigated sample.

### Magnetic Properties

Room-temperature magnetic properties of  $\text{Cd}_x\text{Ni}_{1-x}\text{Zn}_x\text{Fe}_2\text{O}_4$  ( $x = 0.0, 0.2, 0.4$ ) nanoferrites were measured using pulse field hysteresis loop tracer technique by applying a magnetic field of 1000 Oe. Using  $M-H$  plots (Figure) of nanoferrites, the saturation magnetization ( $M_s$ ), remanence magnetization ( $M_r$ ), coercivity ( $H_c$ ), and squareness ratio ( $M_r/M_s$ ) were determined. From Table 1 it is evident that magnetic parameters of CNZ nanoferrites decrease as a function of cadmium content which is associated with linkage between (A) and [B] sites. It may be due to the fact that nonmagnetic  $\text{Cd}^{2+}$  ions ( $0 M_B$ ) replace magnetic  $\text{Ni}^{2+}$  ions ( $2M_B$ )<sup>6</sup>. The magneton number increases up to  $x=0.2$  and then decreases with increasing  $\text{Cd}^{2+}$  content.

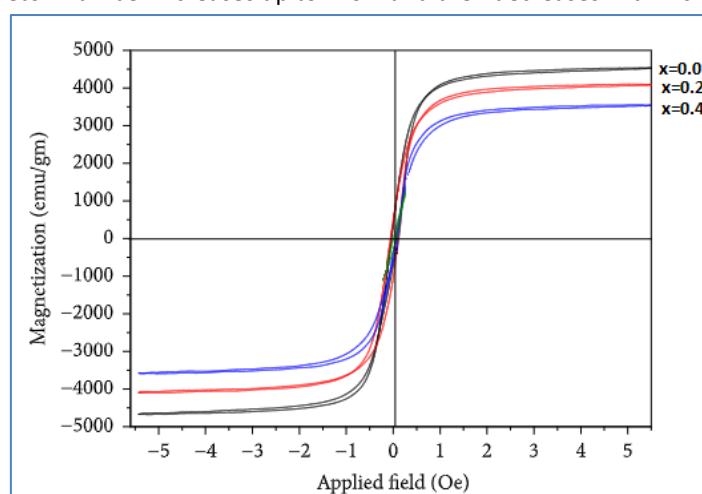


Figure 4: Magnetic hysteresis loops of  $\text{Cd}_x\text{Ni}_{1-x}\text{Zn}_x\text{Fe}_2\text{O}_4$  ( $x = 0.0, 0.2, 0.4$ .)

### Conclusion

X-ray diffraction pattern of the prepared samples confirms the formation of single phase cubic spinel structure. By the substitution of Cd in the Ni-Zn ferrite system, the lattice parameter is decreases and the crystallite size of the sample was in the range 37-42 nm. X-ray density of the samples increases with Cd Substitution. SEM micrographs of the various compositions indicate the morphology of the particles was similar. They are largely agglomerated. The ferrite with composition  $X = 0.0$  shows highest value of saturation magnetization and magnetic moment.

### References

- [1]. B. Jeyadevan, K. Tohji and K. Nakatsuka, J. Appl.Phys. 76 (1994) 6325.
- [2]. L. Darmann, D. Fiarani Magnetic properties of fine particles North Holland, Amsterdam, 1992.
- [3]. Sinthiya, M. M. A., Ramamurthi, K., Mathuri, S., Manimozhi, T., Kumaresan, N., Margoni, M. M., Karthika, P.C., 2014-2015. Synthesis of Zinc Ferrite ( $\text{ZnFe}_2\text{O}_4$ ) Nanoparticles with Different Capping Agents. Int.J. ChemTech Res. 7(5), 2144-2149.
- [4]. S. E. Shirsath, B. G. Toksha and K. M. Jadhav, Structural and Magnetic Properties of  $\text{In}^{3+}$  Substituted  $\text{NiFe}_2\text{O}_4$ , J. Materials Chemistry and Physics, 117(1), 2009,163-168
- [5]. M. Mozaffari, J. Amighian, E. Darsheshdar, Magnetic and structural studies of Nickel – substituted cobalt ferrite nanoparticles, synthesized by sol-gel method' Journal of Magnetism and Magnetic materials, 350, 2014,19-22
- [6]. A. Goldman, Modern Ferrite Technology, (Van Nostrand Reinhold, New York, 1990)
- [7]. S. ManjuraHoque, Md. Amanullah Choudhury and Md.Fakhrul Islam, Characterization of Ni-Cu Mixed

- 
- Spinel Ferrite, Journal of Magnetism and Magnetic Materials, 251(3), 2002, 292-303
- [8]. M. Siva Ram Prasad, B.B.V.S.V. Prasad, B. Rajesh b, K.H. Rao and K.V. Ramesh, "Magnetic Properties and Dc Electrical Resistivity Studies On Cadmium Substituted Nickel-Zinc Ferrite System", Journal of Magnetism and Magnetic Materials, 323, 2011, 2115-2121.
- [9]. R.F. Strickland-Constable, Kinetics and Mechanism of Crystallization, Academic Press, New York, 1968
- [10]. L.H. Gul, J. Magn. Mater., 320, 2008, 270-275
- [11]. Sagar.E. Shirsath, S.M. Patange, R.H. Kadam, M.L. Mane, K.M. Jadhav, J. Mol. Struct. 1024, 2012, 77.
-